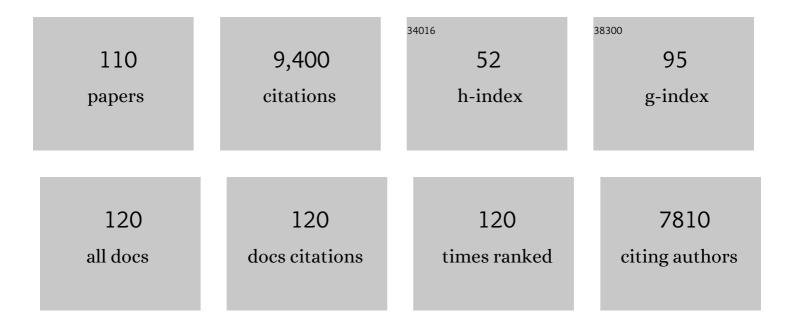
## Rudi Glockshuber

List of Publications by Year in descending order

Source: https://exaly.com/author-pdf/8770119/publications.pdf Version: 2024-02-01



#	Article	IF	CITATIONS
1	NMR structure of the mouse prion protein domain PrP(121–231). Nature, 1996, 382, 180-182.	13.7	1,201
2	NMR characterization of the full-length recombinant murine prion protein, m PrP(23-231). FEBS Letters, 1997, 413, 282-288.	1.3	659
3	Uroplakin Ia is the urothelial receptor for uropathogenic <i>Escherichia coli</i> : evidence from in vitro FimH binding. Journal of Cell Science, 2001, 114, 4095-4103.	1.2	311
4	Influence of Amino Acid Substitutions Related to Inherited Human Prion Diseases on the Thermodynamic Stability of the Cellular Prion Proteinâ€. Biochemistry, 1999, 38, 3258-3267.	1.2	304
5	The structure of a cytolytic α-helical toxin pore reveals its assembly mechanism. Nature, 2009, 459, 726-730.	13.7	303
6	Amyloid-β Aggregation. Neurodegenerative Diseases, 2007, 4, 13-27.	0.8	290
7	Redox properties of protein disulfide isomerase (dsba) from <i>escherichia coli</i> . Protein Science, 1993, 2, 717-726.	3.1	250
8	Atomicâ€Resolution Threeâ€Dimensional Structure of Amyloid β Fibrils Bearing the Osaka Mutation. Angewandte Chemie - International Edition, 2015, 54, 331-335.	7.2	245
9	Exploring the 3D Molecular Architecture of Escherichia coli Type 1 Pili. Journal of Molecular Biology, 2002, 323, 845-857.	2.0	213
10	Recombinant full-length murine prion protein, m PrP(23-231): purification and spectroscopic characterization. FEBS Letters, 1997, 413, 277-281.	1.3	176
11	A single dipeptide sequence modulates the redox properties of a whole enzyme family. Folding & Design, 1998, 3, 161-171.	4.5	174
12	Oligosaccharyltransferase: the central enzyme of Nâ€linked protein glycosylation. Journal of Inherited Metabolic Disease, 2011, 34, 869-878.	1.7	170
13	ERp57 Is a Multifunctional Thiol-Disulfide Oxidoreductase. Journal of Biological Chemistry, 2004, 279, 18277-18287.	1.6	169
14	Characterization of <i>Escherichia coli</i> thioredoxin variants mimicking the activeâ€sites of other thiol/disulfide oxidoreductases. Protein Science, 1998, 7, 1233-1244.	3.1	167
15	Catch-bond mechanism of the bacterial adhesin FimH. Nature Communications, 2016, 7, 10738.	5.8	164
16	The Recombinant Amyloid-β Peptide Aβ1–42 Aggregates Faster and Is More Neurotoxic than Synthetic Aβ1–42. Journal of Molecular Biology, 2010, 396, 9-18.	2.0	145
17	A novel strategy for inhibition of α-amylases: yellow meal worm α-amylase in complex with the Ragi bifunctional inhibitor at 2.5 å resolution. Structure, 1998, 6, 911-921.	1.6	133
18	Structural basis and kinetics of inter- and intramolecular disulfide exchange in the redox catalyst DsbD. EMBO Journal, 2004, 23, 1709-1719.	3.5	122

#	Article	IF	CITATIONS
19	Circularly permuted variants of the green fluorescent protein. FEBS Letters, 1999, 457, 283-289.	1.3	120
20	Random circular permutation of DsbA reveals segments that are essential for protein folding and stability 1 1Edited by R. Huber. Journal of Molecular Biology, 1999, 286, 1197-1215.	2.0	119
21	Extremely rapid folding of the C-terminal domain of the prion protein without kinetic intermediates. Nature Structural Biology, 1999, 6, 550-553.	9.7	118
22	Oxidoreductase activity of oligosaccharyltransferase subunits Ost3p and Ost6p defines site-specific glycosylation efficiency. Proceedings of the National Academy of Sciences of the United States of America, 2009, 106, 11061-11066.	3.3	117
23	Crystal structure of yellow meal worm α-amylase at 1.64 à resolution. Journal of Molecular Biology, 1998, 278, 617-628.	2.0	116
24	The Redox Properties of Protein Disulfide Isomerase (DsbA) of Escherichia coli Result from a Tense Conformation of its Oxidized Form. Journal of Molecular Biology, 1993, 233, 559-566.	2.0	110
25	Reconstitution of Pilus Assembly Reveals a Bacterial Outer Membrane Catalyst. Science, 2008, 320, 376-379.	6.0	110
26	Cytotoxin ClyA from Escherichia coli assembles to a 13-meric pore independent of its redox-state. EMBO Journal, 2006, 25, 2652-2661.	3.5	108
27	Pilus chaperone FimC-adhesin FimH interactions mapped by TROSY-NMR. Nature Structural Biology, 1999, 6, 336-339.	9.7	104
28	Pilus chaperones represent a new type of protein-folding catalyst. Nature, 2004, 431, 329-333.	13.7	102
29	Determination of the Three-Dimensional Structure of the Bifunctional .alphaAmylase/Trypsin Inhibitor from Ragi Seeds by NMR Spectroscopy. Biochemistry, 1995, 34, 8281-8293.	1.2	101
30	Structural basis of chaperone–subunit complex recognition by the type 1 pilus assembly platform FimD. EMBO Journal, 2005, 24, 2075-2086.	3.5	100
31	Bacterial protein disulfide isomerase: Efficient catalysis of oxidative protein folding at acidic pH. Biochemistry, 1993, 32, 12251-12256.	1.2	95
32	The assembly dynamics of the cytolytic pore toxin ClyA. Nature Communications, 2015, 6, 6198.	5.8	83
33	Structural analysis of three His32 mutants of DsbA: Support for an electrostatic role of His32 in DsbA stability. Protein Science, 1997, 6, 1893-1900.	3.1	82
34	Architecture and function of human uromodulin filaments in urinary tract infections. Science, 2020, 369, 1005-1010.	6.0	81
35	Efficient Catalysis of Disulfide Formation During Protein Folding with a Single Active-site Cysteine. Journal of Molecular Biology, 1995, 247, 28-33.	2.0	79
36	Structural Basis of Substrate Specificity of Human Oligosaccharyl Transferase Subunit N33/Tusc3 and Its Role in Regulating Protein N-Glycosylation. Structure, 2014, 22, 590-601.	1.6	78

#	Article	IF	CITATIONS
37	Localization of uroplakin Ia, the urothelial receptor for bacterial adhesin FimH, on the six inner domains of the 16 nm urothelial plaque particle 1 1Edited by W. Baumeister. Journal of Molecular Biology, 2002, 317, 697-706.	2.0	77
38	Autonomous and Reversible Folding of a Soluble Amino-terminally Truncated Segment of the Mouse Prion Protein. Journal of Molecular Biology, 1996, 261, 614-619.	2.0	76
39	Binding of the Bacterial Adhesin FimH to Its Natural, Multivalent High-Mannose Type Glycan Targets. Journal of the American Chemical Society, 2019, 141, 936-944.	6.6	76
40	Structural Basis and Kinetics of DsbD-Dependent Cytochrome c Maturation. Structure, 2005, 13, 985-993.	1.6	75
41	Identification and Characterization of the Chaperone-Subunit Complex-binding Domain from the Type 1 Pilus Assembly Platform FimD. Journal of Molecular Biology, 2003, 330, 513-525.	2.0	73
42	DsbL and DsbI Form a Specific Dithiol Oxidase System for Periplasmic Arylsulfate Sulfotransferase in Uropathogenic Escherichia coli. Journal of Molecular Biology, 2008, 380, 667-680.	2.0	71
43	Quenching of Tryptophan Fluorescence by the Active-Site Disulfide Bridge in the DsbA Protein fromEscherichia coliâ€. Biochemistry, 1997, 36, 6391-6400.	1.2	69
44	DsbA and DsbC-catalyzed Oxidative Folding of Proteins with Complex Disulfide Bridge Patterns In Vitro and In Vivo. Journal of Molecular Biology, 2003, 325, 495-513.	2.0	68
45	Infinite Kinetic Stability against Dissociation of Supramolecular Protein Complexes through Donor Strand Complementation. Structure, 2008, 16, 631-642.	1.6	68
46	Importance of Redox Potential for the in Vivo Function of the Cytoplasmic Disulfide Reductant Thioredoxin from Escherichia coli. Journal of Biological Chemistry, 1999, 274, 25254-25259.	1.6	65
47	Characterization of Recombinant, Membrane-attached Full-length Prion Protein. Journal of Biological Chemistry, 2004, 279, 25058-25065.	1.6	59
48	Mechanism of the electron transfer catalyst DsbB from Escherichia coli. EMBO Journal, 2003, 22, 3503-3513.	3.5	57
49	Staphylococcus aureus DsbA Does Not Have a Destabilizing Disulfide. Journal of Biological Chemistry, 2008, 283, 4261-4271.	1.6	56
50	Mechanism of fibre assembly through the chaperone–usher pathway. EMBO Reports, 2006, 7, 734-738.	2.0	55
51	Structure of Reduced DsbA fromEscherichiacoliin Solutionâ€,‡. Biochemistry, 1998, 37, 6263-6276.	1.2	54
52	Influence of the pKavalue of the buried, active-site cysteine on the redox properties of thioredoxin-like oxidoreductases. FEBS Letters, 2000, 477, 21-26.	1.3	52
53	Structure, Folding and Stability of FimA, the Main Structural Subunit of Type 1 Pili from Uropathogenic Escherichia coli Strains. Journal of Molecular Biology, 2011, 412, 520-535.	2.0	49
54	Uropathogenic E. coli Adhesin-Induced Host Cell Receptor Conformational Changes: Implications in Transmembrane Signaling Transduction. Journal of Molecular Biology, 2009, 392, 352-361.	2.0	48

#	Article	IF	CITATIONS
55	Elimination of All Charged Residues in the Vicinity of the Active-site Helix of the Disulfide Oxidoreductase DsbA. Journal of Biological Chemistry, 1997, 272, 21692-21699.	1.6	47
56	Chaperone-independent Folding of Type 1 Pilus Domains. Journal of Molecular Biology, 2002, 322, 827-840.	2.0	47
57	FRET-based in Vivo Screening for Protein Folding and Increased Protein Stability. Journal of Molecular Biology, 2003, 327, 239-249.	2.0	47
58	Quality control of disulfide bond formation in pilus subunits by the chaperone FimC. Nature Chemical Biology, 2012, 8, 707-713.	3.9	46
59	The Cryoelectron Microscopy Structure of the Type 1 Chaperone-Usher Pilus Rod. Structure, 2017, 25, 1829-1838.e4.	1.6	46
60	A Bacterial Thioredoxin-like Protein That Is Exposed to the Periplasm Has Redox Properties Comparable with Those of Cytoplasmic Thioredoxins. Journal of Biological Chemistry, 1995, 270, 26178-26183.	1.6	43
61	Crystal structure of the ternary FimC–FimF <sub>t</sub> –FimD <sub>N</sub> complex indicates conserved pilus chaperone–subunit complex recognition by the usher FimD. FEBS Letters, 2008, 582, 651-655.	1.3	42
62	The Osaka FAD Mutation E22Δ Leads to the Formation of a Previously Unknown Type of Amyloid β Fibrils and Modulates Aβ Neurotoxicity. Journal of Molecular Biology, 2011, 408, 780-791.	2.0	41
63	RBI, a one-domain α-amylase/trypsin inhibitor with completely independent binding sites. FEBS Letters, 1996, 397, 11-16.	1.3	39
64	Structural and Functional Characterization of the Oxidoreductase α-DsbA1 from <i>Wolbachia pipientis</i> . Antioxidants and Redox Signaling, 2009, 11, 1485-1500.	2.5	39
65	The α-amylase from the yellow meal worm: complete primary structure, crystallization and preliminary X-ray analysis. FEBS Letters, 1997, 409, 109-114.	1.3	37
66	Influence of Acidic Residues and the Kink in the Active-site Helix on the Properties of the Disulfide Oxidoreductase DsbA. Journal of Biological Chemistry, 1997, 272, 189-195.	1.6	36
67	High-resolution Structures of Escherichia coli cDsbD in Different Redox States: A Combined Crystallographic, Biochemical and Computational Study. Journal of Molecular Biology, 2006, 358, 829-845.	2.0	36
68	Preparation and structure of the chargeâ€ŧransfer intermediate of the transmembrane redox catalyst DsbB. FEBS Letters, 2008, 582, 3301-3307.	1.3	34
69	How Periplasmic Thioredoxin TlpA Reduces Bacterial Copper Chaperone Scol and Cytochrome Oxidase Subunit II (CoxB) Prior to Metallation*. Journal of Biological Chemistry, 2014, 289, 32431-32444.	1.6	32
70	Assembly mechanism of the α-pore–forming toxin cytolysin A from <i>Escherichia coli</i> . Philosophical Transactions of the Royal Society B: Biological Sciences, 2017, 372, 20160211.	1.8	31
71	The PAPS-Independent Aryl Sulfotransferase and the Alternative Disulfide Bond Formation System in Pathogenic Bacteria. Antioxidants and Redox Signaling, 2010, 13, 1247-1259.	2.5	28
72	Replacement of Pro109by His in TlpA, a thioredoxin-like protein fromBradyrhizobium japonicum, alters its redox properties but not its in vivo functions. FEBS Letters, 1997, 406, 249-254.	1.3	27

#	Article	IF	CITATIONS
73	Thermodynamic Aspects of DsbD-Mediated Electron Transport. Journal of Molecular Biology, 2008, 380, 783-788.	2.0	27
74	NMR Structure of the Escherichia coli Type 1 Pilus Subunit FimF and Its Interactions with Other Pilus Subunits. Journal of Molecular Biology, 2008, 375, 752-763.	2.0	26
75	(4 <i>R</i> )―and (4 <i>S</i> )â€Fluoroproline in the Conserved <i>cis</i> â€Prolyl Peptide Bond of the Thioredoxin Fold: Tertiary Structure Context Dictates Ring Puckering. ChemBioChem, 2013, 14, 1053-1057.	1.3	26
76	The cryo-EM structure of the human uromodulin filament core reveals a unique assembly mechanism. ELife, 2020, 9, .	2.8	26
77	Folding dynamics and energetics of recombinant prion proteins. Advances in Protein Chemistry, 2001, 57, 83-105.	4.4	23
78	Prion protein structural features indicate possible relations to signal peptidases. FEBS Letters, 1998, 426, 291-296.	1.3	22
79	Acceleration of protein folding by four orders of magnitude through a single amino acid substitution. Scientific Reports, 2015, 5, 11840.	1.6	22
80	Competition between DsbA-Mediated Oxidation and Conformational Folding of RTEM1 β-Lactamase. Biochemistry, 1996, 35, 11386-11395.	1.2	20
81	Structural basis and mechanism for metallochaperone-assisted assembly of the Cu <sub>A</sub> center in cytochrome oxidase. Science Advances, 2019, 5, eaaw8478.	4.7	20
82	Folding and intrinsic stability of deletion variants of PrP(121–231), the folded C-terminal domain of the prion protein. Biophysical Chemistry, 2002, 96, 293-303.	1.5	18
83	Kinetics of the Intramolecular Disulfide Exchange Between the Periplasmic Domains of DsbD. Journal of Molecular Biology, 2007, 367, 1162-1170.	2.0	17
84	Thioredoxinâ€ <b>l</b> ike protein TlpA from <i>Bradyrhizobium japonicum</i> is a reductant for the copper metallochaperone Scol. FEBS Letters, 2012, 586, 4094-4099.	1.3	17
85	Direct Evidence for Self-Propagation of Different Amyloid-Î <sup>2</sup> Fibril Conformations. Neurodegenerative Diseases, 2014, 14, 151-159.	0.8	17
86	The Redox State Regulates the Conformation of Rv2466c to Activate the Antitubercular Prodrug TP053. Journal of Biological Chemistry, 2015, 290, 31077-31089.	1.6	17
87	Characterization of FimC, a Periplasmic Assembly Factor for Biogenesis of Type 1 Pili inEscherichia coliâ€. Biochemistry, 2000, 39, 11564-11570.	1.2	16
88	Solid-state NMR sequential assignment of Osaka-mutant amyloid-beta (Aβ1â^'40 E22Δ) fibrils. Biomolecular NMR Assignments, 2015, 9, 7-14.	0.4	16
89	Glycan–protein interactions determine kinetics of <i>N</i> -glycan remodeling. RSC Chemical Biology, 2021, 2, 917-931.	2.0	16
90	Functional analyses of ancestral thioredoxins provide insights into their evolutionary history. Journal of Biological Chemistry, 2019, 294, 14105-14118.	1.6	15

#	Article	IF	CITATIONS
91	Quantitative Analysis of Nonequilibrium, Denaturant-Dependent Protein Folding Transitions. Journal of the American Chemical Society, 2007, 129, 8938-8939.	6.6	13
92	Evidence for Proton Shuffling in a Thioredoxin-Like Protein during Catalysis. Journal of Molecular Biology, 2008, 382, 978-986.	2.0	13
93	Intramolecular Donor Strand Complementation in the E. coli Type 1 Pilus Subunit FimA Explains the Existence of FimA Monomers As Off-Pathway Products of Pilus Assembly That Inhibit Host Cell Apoptosis. Journal of Molecular Biology, 2014, 426, 542-549.	2.0	13
94	Characterization of Variants of the Pore-Forming Toxin ClyA from <i>Escherichia coli</i> Controlled by a Redox Switch. Biochemistry, 2014, 53, 6357-6369.	1.2	13
95	Acceleration of the Rateâ€Limiting Step of Thioredoxin Folding by Replacement of its Conserved <i>cis</i> â€Proline with (4 <i>S</i> )â€Fluoroproline. ChemBioChem, 2015, 16, 2162-2166.	1.3	13
96	Structure of native glycolipoprotein filaments in honeybee royal jelly. Nature Communications, 2020, 11, 6267.	5.8	13
97	Randomization of the Entire Active-site Helix α1 of the Thiol-disulfide Oxidoreductase DsbA from Escherichia coli. Journal of Biological Chemistry, 2002, 277, 43050-43057.	1.6	12
98	Soluble Oligomers of the Pore-forming Toxin Cytolysin A from Escherichia coli Are Off-pathway Products of Pore Assembly. Journal of Biological Chemistry, 2016, 291, 5652-5663.	1.6	10
99	The Most Stable Protein–Ligand Complex: Applications for Oneâ€Step Affinity Purification and Identification of Protein Assemblies. Angewandte Chemie - International Edition, 2012, 51, 4474-4478.	7.2	7
100	Biochemical pathway for the biosynthesis of the Cu <sub>A</sub> center in bacterial cytochrome <i>c</i> oxidase. FEBS Letters, 2019, 593, 2977-2989.	1.3	7
101	Development of the Mitochondrial Intermembrane Space Disulfide Relay Represents a Critical Step in Eukaryotic Evolution. Molecular Biology and Evolution, 2019, 36, 742-756.	3.5	7
102	Alternative folding to a monomer or homopolymer is a common feature of the type 1 pilus subunit FimA from enteroinvasive bacteria. Journal of Biological Chemistry, 2019, 294, 10553-10563.	1.6	7
103	A metabolite binding protein moonlights as a bileâ€responsive chaperone. EMBO Journal, 2020, 39, e104231.	3.5	6
104	Mechanism of the Prokaryotic Transmembrane Disulfide Reduction Pathway and Its Inâ€Vitro Reconstitution from Purified Components. Angewandte Chemie - International Edition, 2012, 51, 6900-6903.	7.2	3
105	Donor strand sequence, rather than donor strand orientation, determines the stability and non-equilibrium folding of the type 1 pilus subunit FimA. Journal of Biological Chemistry, 2020, 295, 12437-12448.	1.6	3
106	Accelerating the Association of the Most Stable Protein–Ligand Complex by More than Two Orders of Magnitude. Angewandte Chemie - International Edition, 2016, 55, 9350-9355.	7.2	1
107	The trans-to-cis proline isomerization in E.Âcoli Trx folding is accelerated by trans prolines. Biophysical Journal, 2021, 120, 5207-5218.	0.2	1
108	Innenrücktitelbild: Der stabilste Protein-Liganden-Komplex: Anwendung für die Einschritt-Affinitäreinigung und Identifizierung von Proteinkomplexen (Angew. Chem. 18/2012). Angewandte Chemie, 2012, 124, 4569-4569.	1.6	0

#	Article	IF	CITATIONS
109	Inside Back Cover: The Most Stable Protein-Ligand Complex: Applications for One-Step Affinity Purification and Identification of Protein Assemblies (Angew. Chem. Int. Ed. 18/2012). Angewandte Chemie - International Edition, 2012, 51, 4491-4491.	7.2	Ο
110	Accelerating the Association of the Most Stable Protein–Ligand Complex by More than Two Orders of Magnitude. Angewandte Chemie, 2016, 128, 9496-9501.	1.6	0